

Supporting Information

Broadening Spectral Response and Achieving Environmental Stability in SnS₂/Ag-NPs/HfO₂ Flexible Phototransistor

Muhammad Farooq Khan^{1#}, Sana Sadaqat^{2#}, Muhammad Asghar Khan^{3#}, Shania Rehman⁴,
Waqas Subhani⁵, Mohamed Ouladsmane⁶, Malik Abdul Rehman⁷, Fida Ali⁸, Harri Lipsanen⁸,
Zhipei Sun⁸, Jonghwa Eom^{3*} and Faisal Ahmed^{8*}

¹Department of Electrical Engineering, Sejong University, Seoul 05006, Republic of Korea.

²Department of Physics, Riphah International University, Faisalabad Campus, Pakistan.

³Department of Physics and Astronomy, Sejong University, Seoul 05006, Republic of Korea.

⁴Department of Semiconductor System Engineering, Sejong University, Seoul 05006, Republic of Korea.

⁵Department of Physics University of Lahore, Lahore, 53700, Pakistan

⁶Department of Chemistry, College of Science, King Saud University, Riyadh, 11451, Saudi Arabia.

⁷Department of Chemical Engineering, New Uzbekistan University, Tashkent, 100007, Uzbekistan

⁸Department of Electronics and Nano engineering, Aalto University, P.O. Box 13500, FI-00076 Aalto,
Finland.

These authors contributed equally

Corresponding authors: faisal.ahmed@aalto.fi and eom@sejong.ac.kr

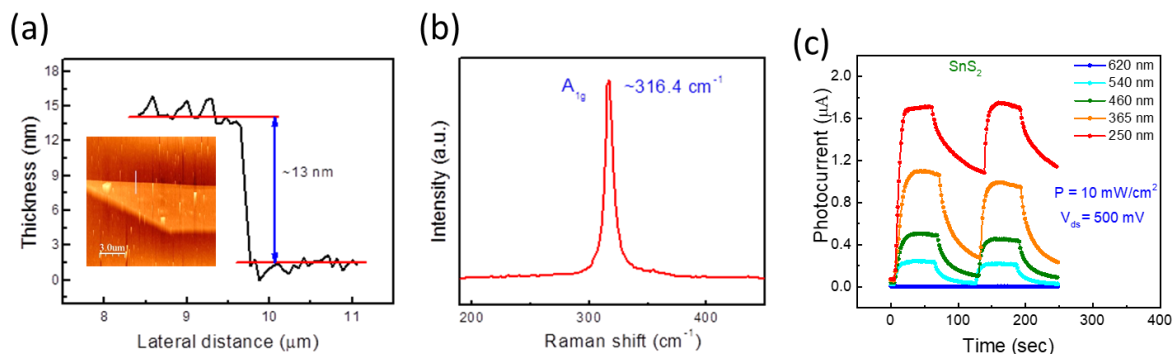


Figure S1: Characterization of SnS₂ device. (a) Thickness profile of SnS₂ device obtained by atomic force microscopy. Inset: topographic image of SnS₂ flake. (b) Room temperature Raman spectrum of SnS₂ flake depicting single A_{1g} peak. (c) Time-dependent photocurrent of SnS₂ device.

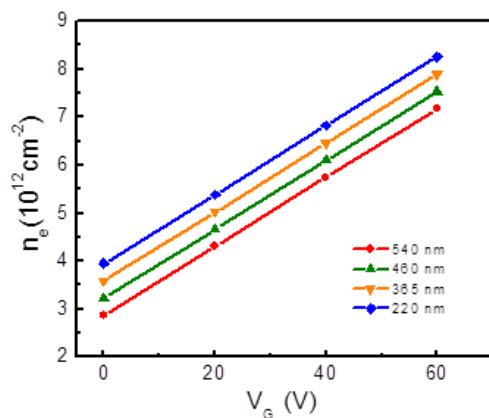


Figure S2: Carrier concentration at different gating conditions. The electron concentration [$n_e = C_{ox}(V_g - V_{th})$] at V_g values (0, 20, 40, and 60V) is calculated, and it shows an increasing trend as we irradiate the lower wavelength light. This demonstrates that the devices under light having lower (higher) wavelengths generate large (small) carriers, which can improve the charge density and field-effect mobility of the SnS₂ transistor.

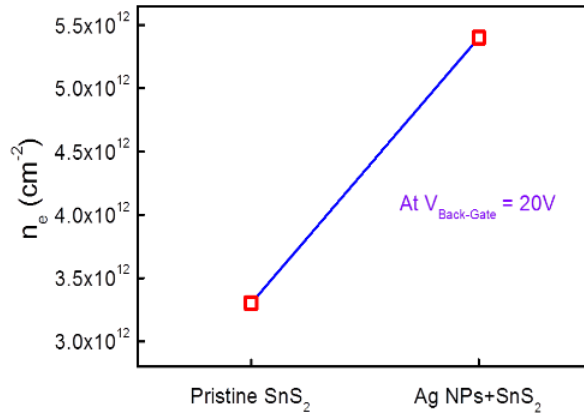


Figure S3: Comparison of carrier concentration. The electron carrier density of pristine SnS_2 and $\text{SnS}_2+\text{Ag}(\text{NPs})$ at $V_g = 20\text{V}$.

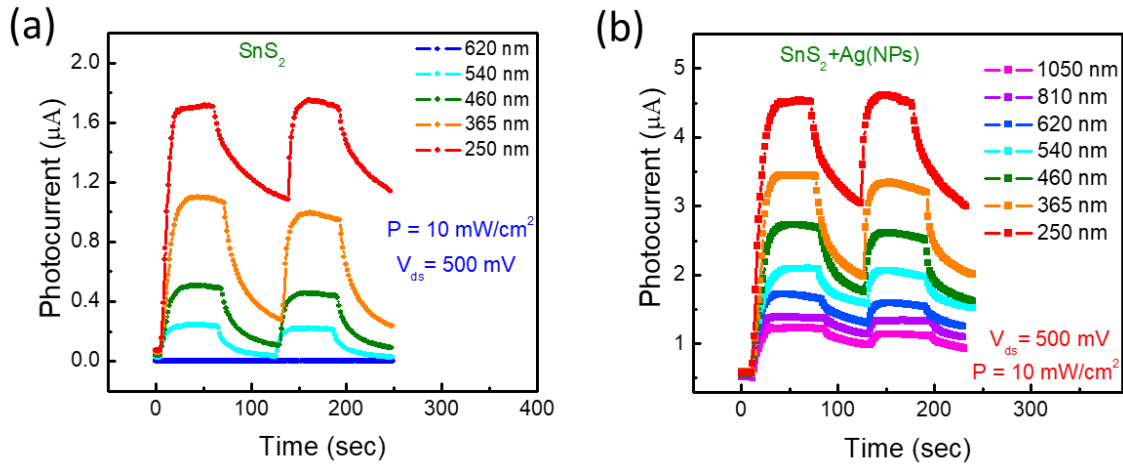


Figure S4: Comparison of temporal photocurrent. The time-dependent photocurrent of pristine SnS_2 and $\text{SnS}_2/\text{Ag-NPs}$ at $V_g = 0\text{V}$ and $V_{ds} = 500\text{mV}$. The light intensity was kept at $10\text{mW}/\text{cm}^2$ during all the wavelength irradiation.

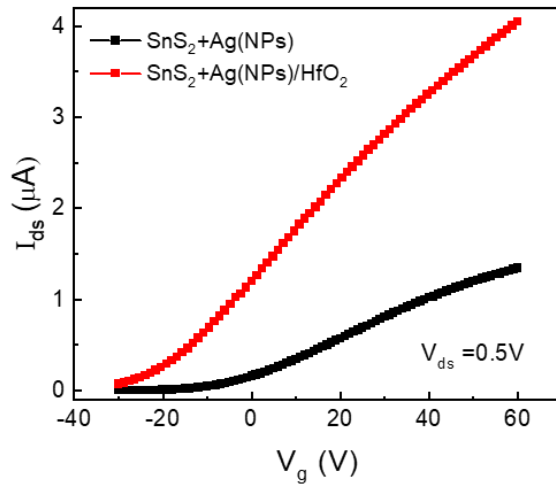


Figure S5: Transfer curve comparison. The transfer curves of SnS₂/Ag-NPs and SnS₂/Ag-NPs/HfO₂ transistors.

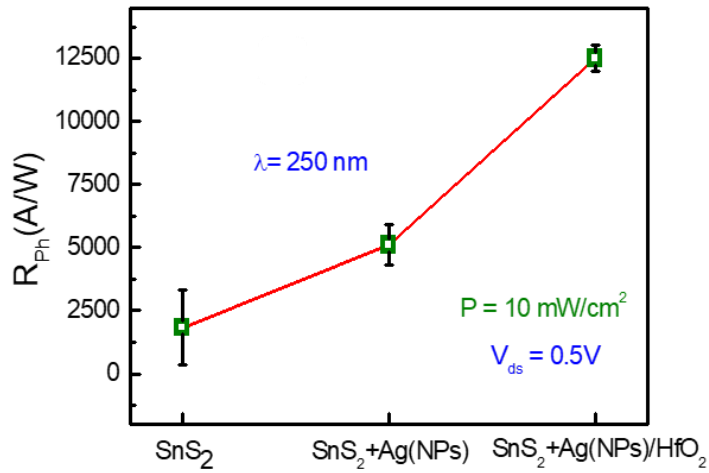


Figure S6: Enhancement in photoresponsivity for different device configuration. The comparative photoresponsivity of SnS₂, SnS₂/Ag-NPs and SnS₂/Ag-NPs/HfO₂ photodetectors at $V_g = 0V$.

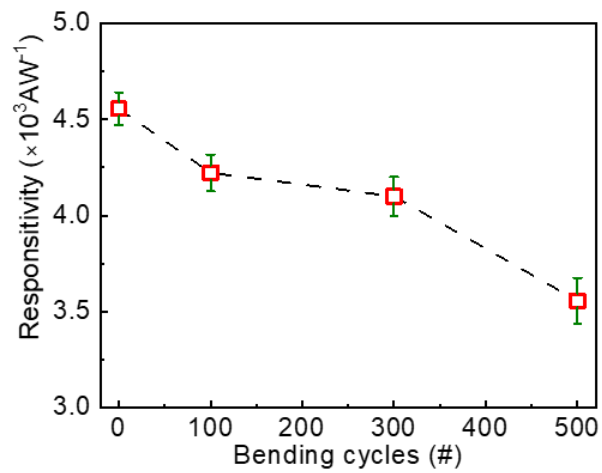


Figure S7: Effect of bending cycles on photoresponsivity. The responsivity of flexible SnS₂/Ag-NPs photodetector for repeated bending cycles at $\lambda = 250 \text{ nm}$, $P = 10 \text{ mW/cm}^2$.

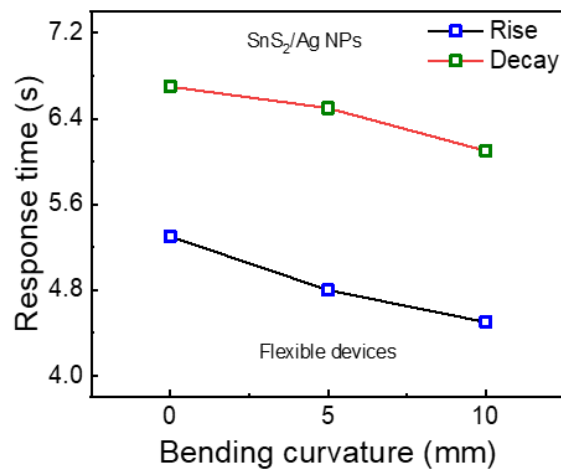


Figure S8. The rise (blue square) and decay (green square) times of SnS₂/Ag-NPs photodetectors under $\lambda = 250 \text{ nm}$ at various bending states.

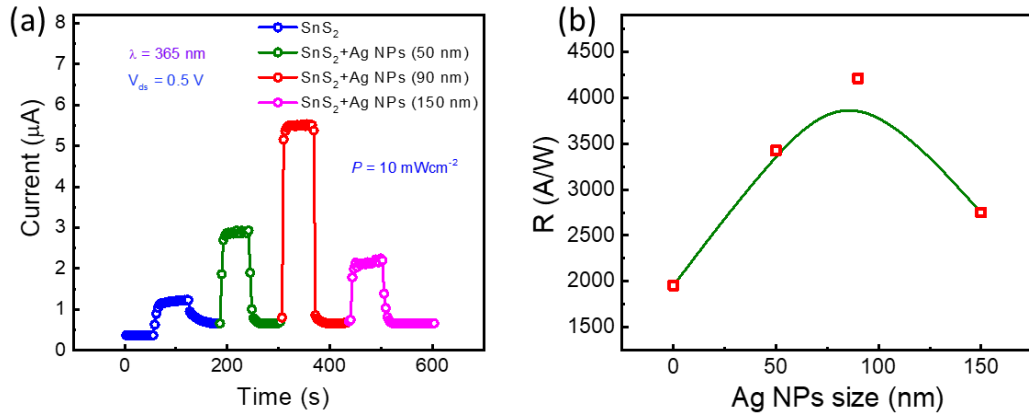


Figure S9. (a) The drain current of SnS₂ photodetectors under light $\lambda = 365$ nm while decorating the different size of Ag NPs. (b) The photoresponsivity of SnS₂ photodetectors at various sizes of Ag NPs.

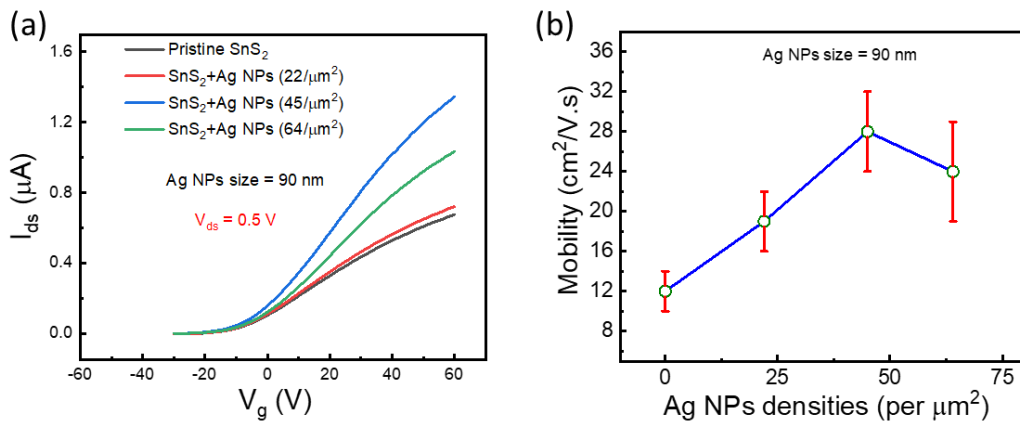


Figure S10. (a) The transfer curves of SnS₂ transistors with decoration of Ag NPs (90 nm) having different densities. (b) Field effect mobilities of SnS₂/Ag NPs (90 nm) transistors with various densities.